Performance Comparison of an ECR Plasma Thruster using Argon and Xenon as Propellant Gas

IEPC-2013-420

Presented at the 33rd International Electric Propulsion Conference,
The George Washington University • Washington, D.C. • USA
October 6 – 10, 2013

Julien Jarrige[1], Paul-Quentin Elias[2], Félix Cannat[3], Denis Packan[4]
ONERA – The French Aerospace Lab, Palaiseau, France

The Electron Cyclotron Resonance (ECR) plasma thruster is an electric propulsion device that combines the high ionization performances of an ECR source and the simultaneous acceleration of electrons and ions in a magnetic nozzle. A coaxial ECR thruster under development at ONERA is tested using xenon and argon as the propellant gas. The influence of mass flow rate and microwave power on ion current and ion energy distribution is evaluated and the performances with the two gases are compared. Mass utilization efficiency up to 45% and ion energy up to 350 eV have been obtained with a microwave power around 50 W for xenon.

Nomenclature

B	=	magnetic field, T
C	=	conductance, L/s
D	=	distance between the probe and the thruster
E_i	=	ion energy, eV
e	=	elementary charge, C
f_{ce}	=	electron cyclotron frequency, Hz
g	=	acceleration of gravity, m/s^2
I_i	=	total ion current, A
I_{sp}	=	specific impulse, s
J_i	=	ion current density, A/m^2
m_e	=	electron mass, kg
M_i	=	ion atomic mass, kg
$\dot{m}_g$	=	propellant gas mass flow rate, kg/s
$\dot{m}_i$	=	ion mass flow rate, kg/s
p_S	=	pressure in ECR source, mbar
P	=	microwave power, W
Q	=	throughput of propellant gas, mbar.L/s
S_{eff}	=	effective pumping speed, L/s
T	=	thrust, N
T_g	=	gas temperature
T_d	=	thrust density, N/m^2
TTP	=	thrust-to-power ratio [mn/W]
ε	=	electron energy, J
v_i	=	ion velocity, m/s
μ	=	magnetic moment, J/T
η_m	=	mass utilization efficiency
η_e	=	energy efficiency

[1] Research Scientist, Physics and Instrumentation Department, julien.jarrige@onera.fr, AIAA member.
[2] Research Scientist, Physics and Instrumentation Department, paul-quentin.elias@onera.fr.
[3] Ph.D. Student, Physics and Instrumentation Department, felix.cannat@onera.fr.
[4] Research Scientist, Physics and Instrumentation Department, denis.packan@onera.fr.

η_D = divergence factor
η_T = thruster efficiency
θ = angle to thruster axis

I. Introduction

Electric propulsion has become widespread for satellites control and deep space scientific missions, where there is a need for propulsion systems with a high specific impulse (I_{sp}). Several technologies have been developed (the most mature being Hall Effect Thruster, Gridded Ion Engine, High Efficiency Multistage Plasma Thruster), which are all based on ionization of a propellant gas in plasma source and electrostatic acceleration of the positive ions with an externally applied electric field. The positive ion beam that exits the thruster then needs to be neutralized with an auxiliary electron emitter to avoid charging of the satellite.

For this reason, quasi-neutral thrusters have gained interest in the last years. Magnetoplasmadynamic (MPD) thrusters have shown the potential for the production of high thrusts with a good efficiency, but the erosion of the electrode could reduce the lifetime of the thruster. Other concepts of electric propulsion have been developped by using a magnetic field to radially confine the plasma and to accelerate simultaneously ions and electrons in the plume. Helicon plasma sources for example have been intensively studied for electric propulsion purposes because of their simple design and their robustness [1,2,3,4,5].

Another electrodeless propulsion system, the Gas Dynamic Mirror (GDM), is based on plasma confinement between two magnetic mirrors [6]. As the ions gain energy and the plasma density increases, the ion-ion mean free path becomes such that the plasma can be considered as a fluid. GDM has been used with electron cyclotron heating from a right-hand circularly polarized wave (RHCP). An ion acceleration region due to ambipolar electric field was identified at the exit of the mirror [7]. Because the principle of the magnetic nozzle is critical in all quasi-neutral thruster technologies, its theoretical study and numerical simulation have been paid a great attention in order to understand how the thrust is produced [8,9,10,11]. The conversion of electron thermal energy into ion kinetic energy by the ambipolar potential has been studied, and several detachment schemes have been proposed.

Finally, the Variable Specific Impulse Magnetoplasma Rocket (VASIMR) combines electron heating in a helicon plasma source and ion cyclotron heating in a resonant RF stage [12]. High temperature electrons and ions are then accelerated in a diverging magnetic nozzle. Unlike previously mentioned quasi-neutral thruster, no ambipolar electric field is necessary to increase the ion velocity and produce a thrust. Recently, the VX-200 engine operated with argon has shown thruster efficiency higher than 50% with a total power of 100 kW [13].

In this paper, we present another type of quasi-neutral electric propulsion system, namely the Electron Cyclotron Resonance (ECR) plasma thruster. Several studies on the application of ECR sources to electric propulsion have been led in the past [14,15,16,17]. They use micro-waves in TE modes (RHCP or planar waves) with high power (several hundreds to several thousands W). The originality of the ECR plasma thruster developed at ONERA lies in its coaxial geometry, its magnetic field configuration and the low power consumption (50 W). The principle of the thruster and its design are presented in section II. Section III describes the experimental setup, the diagnostics used and the thruster performances evaluation parameters for argon and xenon. The experimental results are presented in Section IV, and Section V summarizes the results and gives concluding remarks.

II. Description of ECR thruster

A. Principle of ECR thruster

The thruster is based on electron heating by ECR effects and plasma acceleration in a magnetic nozzle.

In a radially confined magnetized plasma, the electrons gyrate around the field lines at the frequency f_{ce} defined by:

$$f_{ce} = \frac{eB}{2\pi m_e} \quad (1)$$

where B is the magnetic field strength, e the elementary charge and m_e the mass of the electron.

When applying a micro-wave (MW) EM field at the frequency f_{ce}, resonance effects are obtained: the electrons are efficiently heated to high temperatures. Inelastic collisions between electrons and neutral then lead to high ionization of the gas. For a standard magnetron frequency of 2.45 GHz, ECR conditions are met with a magnetic field of 875 Gauss.

In the magnetic nozzle, the acceleration of the charged species rest upon the magnetic mirror principle. The electron gyrokinetic energy is converted to longitudinal kinetic energy under the effect of the divergent magnetic field. This is illustrated by conservation of the electron energy ε and of the magnetic moment μ:

$$\varepsilon = \frac{1}{2} m_e v_{\parallel}^2 + \mu B(z) \quad (2)$$

$$\mu = \frac{m_e v_{\perp}^2}{2B} \quad (3)$$

where $v_{\parallel}$ is the electron longitudinal velocity (parallel to the magnetic field lines), and $v_{\perp}$ is the electron perpendicular velocity (*i.e.* the electron temperature).

Ions, which are much heavier and colder than electrons, are only partially magnetized, so they can be considered as static. A space charge is formed while the electrons exit the thruster, thus producing an electric field that accelerates the ions downstream.

An ECR thruster has two main advantages over existing electric propulsion technologies:

_ the plume is electrically neutral, so there is no need for a cathode neutralizer downstream. Moreover, the plume is not space-charge limited, which theoretically enables to produce very high current density, *i.e.* a high thrust per unit area.

_ the ion acceleration is only due to the ambipolar electric field formed in the magnetic nozzle. Therefore there is no need for accelerating grids and the only power supply that is required is the microwave generator.

B. ECR Source design

The ECR thruster under development at ONERA is based on a compact coaxial geometry [18], as shown in Fig. 1. The coaxial line is connected to an antenna 1.5 mm in diameter and to a cylinder 13 mm in diameter and 15 mm long. A DC-block is inserted on the coaxial line in order to enable the antenna and the cylinder to be floating at their own potential. A dielectric material plate is used to insulate the back of the cavity from the plasma. The gas is injected radially through two tubes 1 mm inner diameter. The electric field generated by the MW power at 2.45 GHz is therefore purely radial in the cavity: only TEM modes are allowed to propagate, with an azimuthal MW magnetic field. The coaxial geometry enables to reduce the size of the thruster: with conventional rectangular or circular waveguides systems, dimensions on the order of magnitude of the wavelength would be required for MW propagation. Coaxial ECR sources have already been successfully used to produce high energy ion beams for molecular beam epitaxy or for ECR ion source (ECRIS) [19,20,21,22], but the process rest upon electrostatic acceleration of ions with grids. Our source is designed to enable the ejection of electrons and ions.

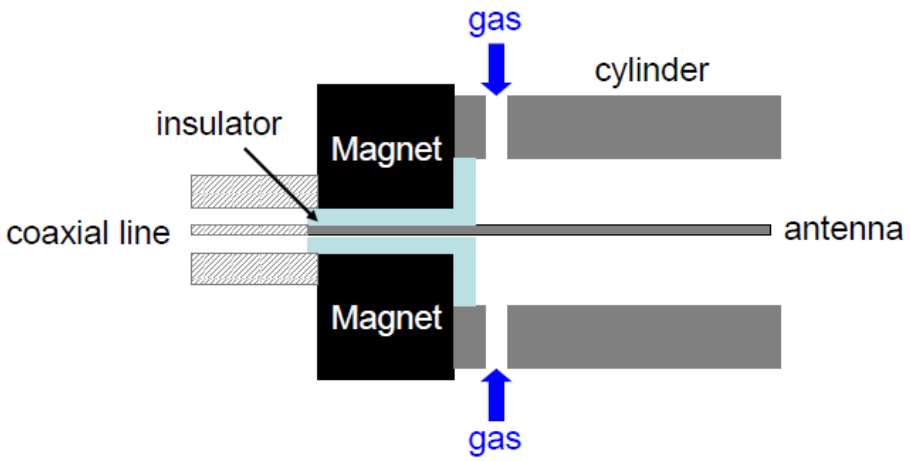

Fig. 1 Schematic diagram of the ECR source.

The resonant magnetic field is provided by a set of Neodyme permanent magnets placed upstream the ECR source. The magnetic field was chosen as to ensure a purely divergent magnetic field in the ECR source and the magnetic nozzle, as shown in Fig. 2. The magnetic field is measured on the source axis with a gaussmeter. The resonant magnetic field at 2.45 GHz, which is indicated by the green line, is the middle of the ECR source (grey region) where the oscillating electric field is applied.

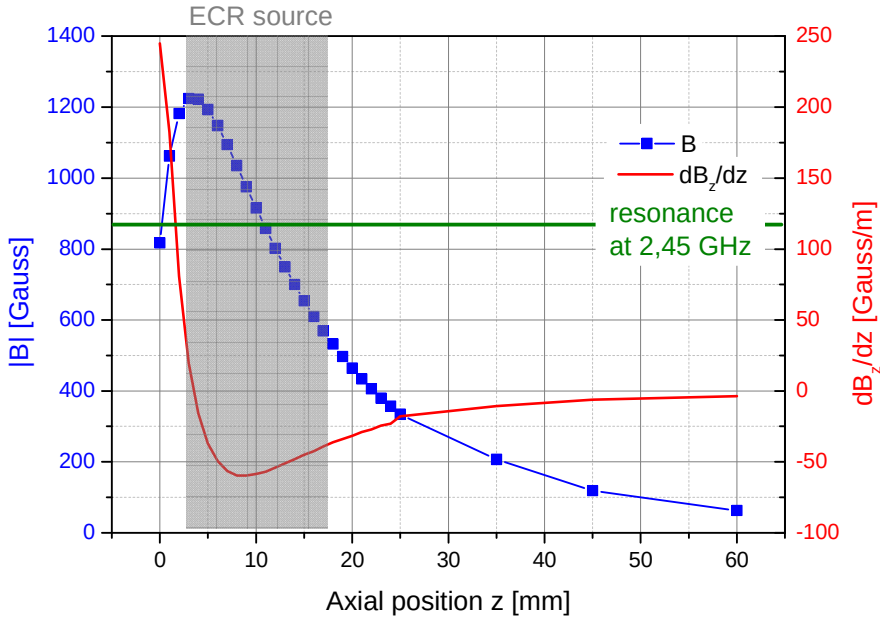

Fig. 2 Axial magnetic field strength B_z and magnetic field gradient dB_z/dz in the electron cyclotron source and the magnetic nozzle.

The resonant magnetic field for the MW frequency of 2.45 GHz is located in the middle of the source. If we consider electrons in gyration around the magnetic field lines in a narrow zone around this resonant field, and assuming that electrons gain energy from the electric field only in this zone, two advantages arise from this magnetic field topology:

_ electrons with a positive longitudinal velocity (with respect to the z axis in Fig. 2) are continuously accelerated downstream by the divergence of the magnetic field.

_ electrons with a negative longitudinal velocity are for the most part reflected by the magnetic field convergence and comes back in the ECR zone where they follow the divergence of the magnetic field. According to equations (2) and (3), the electrons that can travel through the magnetic peak and are collected by the dielectric backplate are such as:

$$\frac{1}{2} m_e v_{\parallel 0}^2 > \mu (B_{bp} - B_0)$$

where $v_{\parallel 0}$ is the initial longitudinal velocity (in the ECR zone), B_{bp} and B_0 are the magnetic field strengths at the location of the backplate and the resonance zone, respectively. This is very unlikely to happen, because the electrons gain only gyrokinetic energy in the resonance process. It is noteworthy that this simple approach does not take into account the ambipolar potential profile.

III. Experimental apparatus

A. Facility

All experiments were carried out in B09 facility at ONERA center of Palaiseau. B09 (Fig 3) is a cylindrical vacuum tank 2 m long and 0.8 m in diameter equipped with three Pfeiffer HiPace 2300 turbomolecular pumps (total pumping speed: 3000 L/s in argon) that ensures a base pressure below 10^{-7} mbar. An MKS 999 Quattro multi-sensor transducer is used to monitor the pressure in the tank. The xenon and argon flow into the thruster is regulated with a Bronkhorst El-Flow mass flow controller. In the conditions of the experiments, the thruster was operated with flow rates in the range [0.06-0.3 mg/s], and the background pressure was [$4\text{x}10^{-6}$-$2\text{x}10^{-5}$ mbar]. The effective pumping speed of the vacuum system is estimated at about 2500 L/s for xenon and 4000 l/s for argon.

The thruster is powered by a SAIREM magnetron source with a fixed frequency (2.45 GHz) and an adjustable output power. A circulator with 50 Ohms load is used to dissipate the reflected power to the generator. The power transmitted to the plasma load was monitored with a bidirectional coupler and diode detectors. It should be mentioned that the forward and reflected power were measured between the generator and the microwave feedthrough on the tank. Therefore the transmitted MW power values indicated in this paper include the power

losses in the cables, the feedthrough, the DC block, and all connectors and adapters. Recent measurements on the microwave chain lead us to estimate the total power attenuation of these components at a level of at least 2 dB.

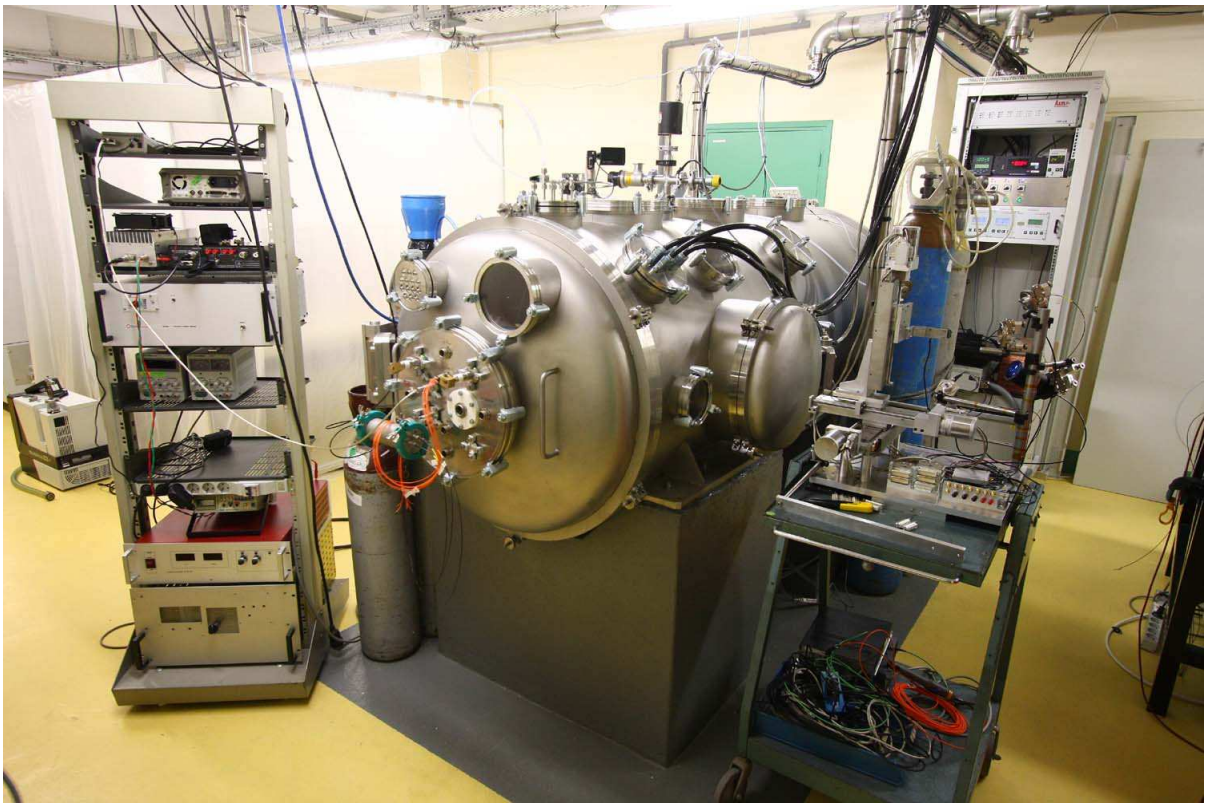

Fig 3. B09 vacuum chamber at ONERA Palaiseau.

B. Plume characterization

The ECR thruster is mounted on a rotation stage inside the vacuum chamber in order to perform angular scans of the plume properties: the total ion current I_i, the angular profile of ion current density $J_i(\theta)$, and the ion energy distribution function (IEDF). These parameters, which are currently measured in plasmas with electrostatic probes, determine the thrust and the efficiency of the propulsion system. However, electrostatic measurements in the ECR plume are made difficult by the properties of the beam that is composed of ions and electrons, both of them with a high energy. Two electrostatic probes were developed for the ECR plume characterization: a gridded Faraday probe for ion current measurements, and a retarding potential analyzer (RPA) for IEDF.

In a standard planar Faraday cup, the collector is biased at a negative potential in order to repell all incoming electrons and to collect only ions. However, in the case of high kinetic energy electrons, the potential to be applied to the collector in order to work in the ion saturation region is so large that it can significantly disturb the plume: a sheath is created around the probe, which increases its effective collection area and leads to an overestimation of ion current. This effect is further increased with a higher electron density in the plume. In order to overcome this problem, a gridded Faraday probe has been developed at ONERA: the collector is placed behind a grid whose potential is floating. The grid acts as an electrostatic screen between the collector and the plume. The collected ion current is measured with a Keithley picoammeter, and the ion current density is then obtained dividing this current by the ion collection aperture (6 mm in diameter), taking into consideration the grid transmission (50%).

The retarding potential analyzer consists of four polarized grids and a collector. The first grid (floating) acts as an electrostatic screen,. The second grid is negatively biased in order to repel all electrons from the plume. The potential of the third grid (analysis grid) is scanned positively to filter the ions as a function of their kinetic energy. The role of the fourth grid is to repel secondary electrons produced by impact of ions on the grids inside the RPA. The ion energy distribution function is then obtained by derivation of collector current versus analysis grid potential.

The 4-grids RPA is well known for IEDF measurement in RF plasmas [23], and has also already been used for the characterization of very high energy ion beams [24], and of quasi-neutral helicon thruster plume [4]. An example of I-V curve obtained with our RPA and the corresponding IEDF are shown in Fig. 4. The results of the RPA were validated using a Hiden PSM Ion Analyzer, which can perform simultaneous scans of energy up to 1000 eV (for a given m/Z) and mass up to 300 amu (for a given ion energy).

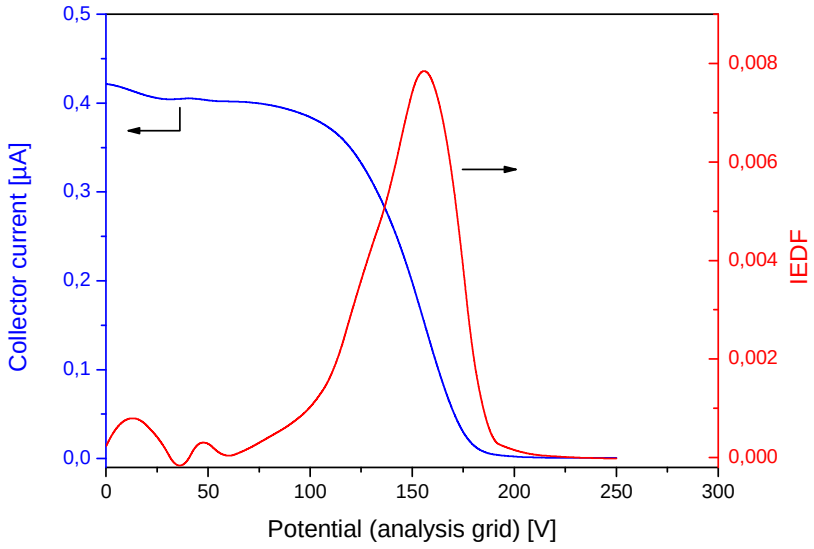

Fig. 4 Typical ion current-voltage curve measured with the RPA (blue) in the thruster plume and corresponding IEDF (red).

The electrostatic probes are installed on a three axis translation stage system that enables to change the measuring probe. The probes are placed at 30 cm from the thruster for all measurements presented in this paper.

C. Performance evaluation

From the experimental measurements (angular profile of ion current density and IEDF), several typical thruster parameters listed below can be calculated [25].

Total ion current I_i is obtained by integration of ion current density $J_i(\theta)$ over the plume profile (assuming the axisymetry of the plume):

$$I_i = \int_{\theta=-\pi/2}^{\pi/2} J_i(\theta)\pi D^2 \sin(\theta) d\theta \qquad (4)$$

where D is the distance between the probe and the thruster, and θ the angle to the thruster axis.

The mass utilization efficiency η_m is the ratio of ion mass flow over gas mass flow. It represents the fraction of propellant gas that is effectively used for the thrust:

$$\eta_m = \frac{I_i M_i}{\dot{m}_g e} = \frac{\dot{m}_i}{\dot{m}_g} \qquad (5)$$

where M_i is the ion atomic mass, and $\dot{m}_g$ is the propellant gas mass flow.

The thrust T can be estimated from the ion current density profile and the mean ion velocity v_i at centerline (assuming that the ion velocity is uniform over the angular profile):

$$T = \int_{\theta=-\pi/2}^{\pi/2} J_i(\theta)\frac{M_i}{e} v_i \pi D^2 \sin(\theta)\cos(\theta) d\theta \quad \text{with } v_i = \sqrt{\frac{2E_i}{M_i}} \qquad (6)$$

where E_i is the mean ion energy determined from the IEDF at centerline.

The energy efficiency η_e compares the power necessary for ion acceleration and the power supplied to the thruster P:

$$\eta_e = \frac{I_i E_i}{P} \qquad (7)$$

The divergence factor η_D is used to correct the divergence of the plume that causes a decrease of the produced thrust:

$$\eta_D = \frac{T}{\dot{m}_i v_i} \qquad (8)$$

The thruster η_T efficiency is defined by:

$$\eta_T = \eta_m \eta_e \eta_D{}^2 = \frac{T^2}{2\dot{m}_g P} \qquad (9)$$

The specific impulse I_{sp} (in seconds), which is the ration of the thrust to the rate of propellant consumption, is another typical measure of the thrust efficiency:

$$I_{sp} = \frac{T}{\dot{m}_g g} \qquad (10)$$

IV. Results

The performance of the ECR thruster was investigated as a function of MW power (up to 51 W) and xenon and argon mass flow rate (between 0.06 and 0.3 mg/s). The MW power that is indicated in this part refers to the transmitted power, *i.e.* the difference between forward and reflected power measured with the coupler. A typical plume produced by the ECR thruster is shown in Fig. 5.

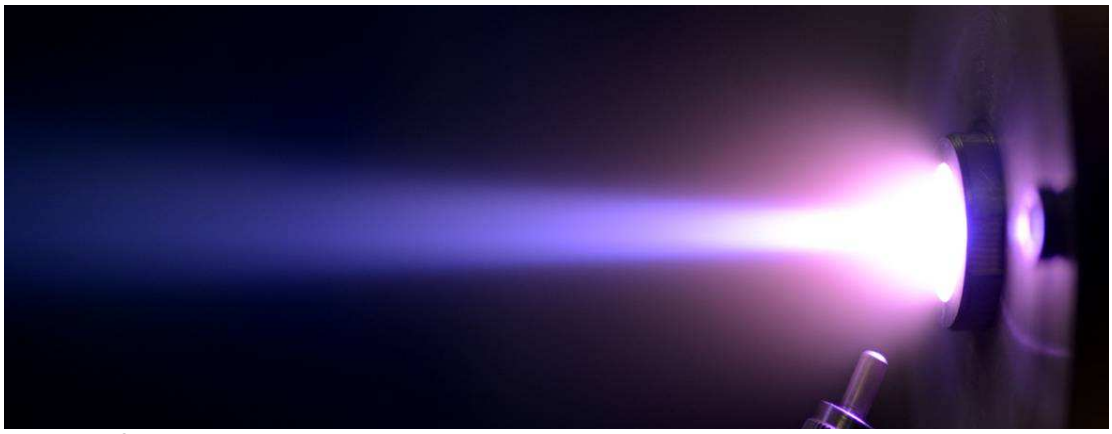

Fig. 5 View of ECR thruster plume in argon.

Fig. 6 shows an example of angular profiles of ion current density measured for different MW powers and mass flow rates. Similar profiles are obtained for all MW powers for both gases, with a constant plume half-angle at current half-maximum around 25°. The ion current density at the center of the plume is seen to increase with MW power.

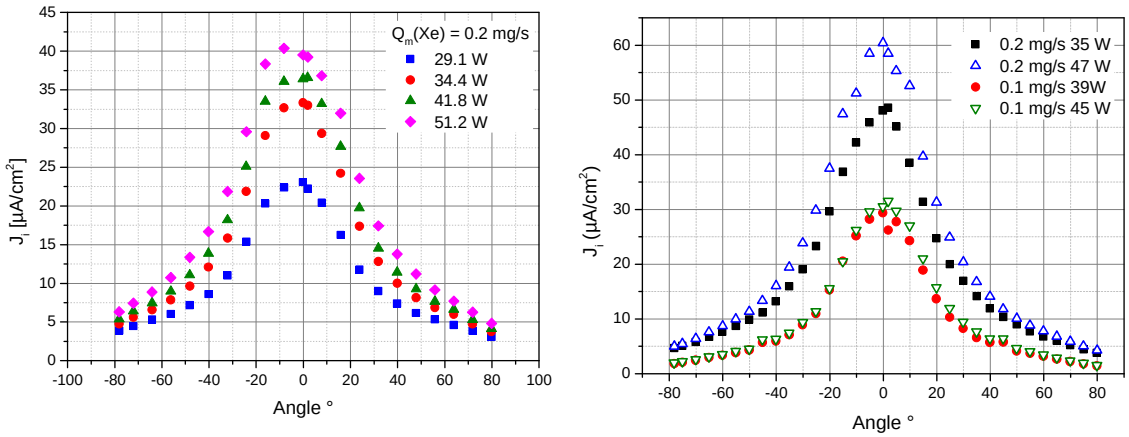

Fig. 6 Angular profile of the ion current density for a xenon (left) and argon (right).

The evolution of total ion current and mass utilization efficiency with the MW power is shown in Fig. 7. For all MW powers, the ion current increases with mass flow. At 0.2 and 0.3 mg/s, I_i increases almost linearly with MW power, while the increase is less significant at 0.1 mg/s for xenon and no effect of the MW power is seen at 0.06 mg/s for xenon. The transmitted power could not be increased above 40 W at this flow rate because of the poor matching of the plasma.

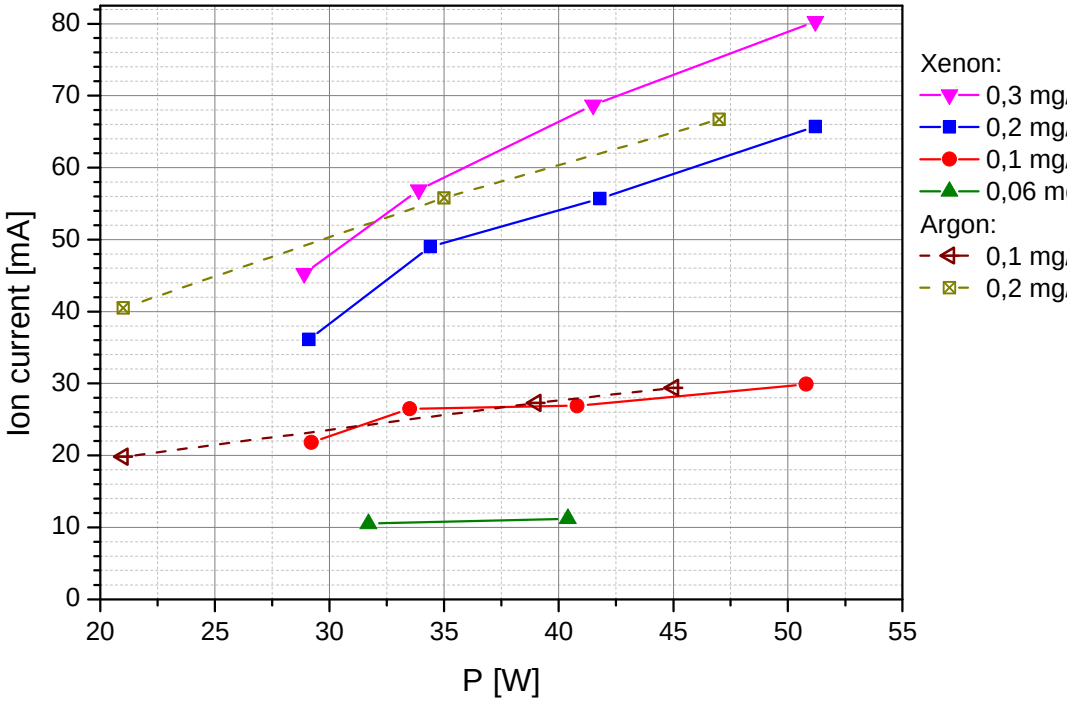

Fig. 7 Total ion current vs MW power for xenon (left) and argon (right). Flow rates are in mg/s.

The mass utilization efficiency is shown for xenon in Fig. 8. Better performances are achieved when the thruster is operated with xenon flow rates of 0.1 and 0.2 mg/s. The highest mass utilization efficiency of 45% is obtained with a mass flow rate of 0.2 mg/s and a power of 51 W. The transmitted power could not be further increased because of heating of the cables and MW components due to losses, but it seems reasonable to think from the curve trend that higher η_m could be reached with higher power.

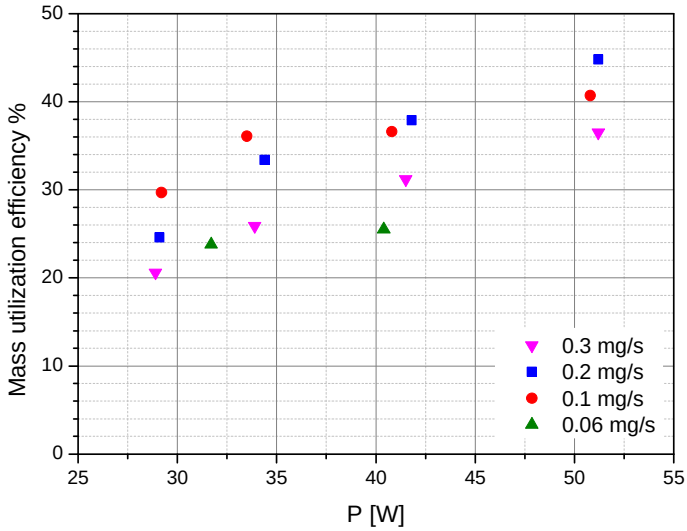

Fig. 8 Mass utilization efficiency of ECR thruster vs MW power for different xenon mass flows.

The energy distribution on the thruster axis strongly depends on the mass flow rate, as illustrated in Fig. 9. All IEDFs are measured for the same MW power transmitted to the load (~36 W for xenon, ~27W for argon). The distributions have a narrow peak of high energy (with a FWHM less than 15 eV), and a smaller peak of low energy at around 10-15 eV. The low energy peak corresponds to slow ions produced in the plume by charge exchange or electron impact of the background gas. The contribution of slow ions to total current is negligible below about 0.2 mg/; at 0.3 mg/s, the background pressure in the tank is high enough to produce a significant effect. The high energy ion peak is shifted to higher energies when the mass flow rate is reduced. The width of the peaks are broader for argon.

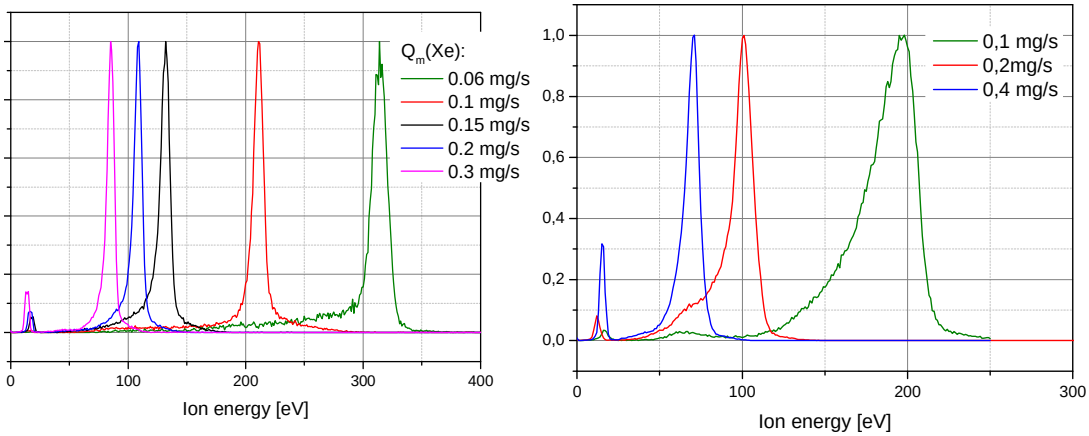

Fig. 9 Dependence of IEDF (normalized) on the xenon mass flow (left) and on the argon mass flow (right).

V. Discussion

A summary of ECR plasma thruster performances is shown in Table 1 for xenon and table 2 for argon. The xenon total efficiencies are typically 3 times higher than for argon. One of the most important results is the high ion energy values measured in the plume of ECR plasma thruster. It is noteworthy that the acceleration of ions is only due to the ambipolar electric field, *i.e.* the conversion of electron temperature into ion kinetic energy in the magnetic nozzle. The influence of the propellant gas mass flow rate could be understood as the effect of the pressure inside the ECR source. As the pressure in the ECR source increases, the collision rate of electrons increases, which results in a decrease of electron gyrokinetic energy. The pressure in the middle of ECR source p_S can be calculated from the effective pumping speed of the turbomolecular pumps S_{eff}, the throughput of gas Q and the conductance of the cylinder C:

$p_S = Q(1/S_{eff} + 1/C)$, with $C = \frac{\pi}{12}\sqrt{\frac{8kT_g}{\pi M}}\frac{D^3}{L}$,

where T_g is the gas propellant temperature, D is the source diameter (13 mm) and L is taken at 10 mm. For xenon mass flow between 0.06 and 0.3 mg/s, the source pressure is found to vary in the range [$8x10^{-4}$ - $4.1x10^{-3}$ mbar].

A comparison with helicon thrusters results show that lower energy values are encountered in these propulsion systems: ion energy in HDLT (operated with various gas) is typically 20 to 50 eV, as reported by the group of Boswell [1,26].Batishchev observed argon ion beams up to 100 eV in the mini-helicon thruster [5], and Wiebold *et al.* measured argon ion energy up to 165 eV in the MadHeX helicon source [4]. Recently, Shabshelowitz and Gallimore developed a kW radio-frequency plasma thruster with an ion energy up to 100 eV [27]. The higher ion energy observed in our ECR plasma thruster is probably due to higher electron energy in the source. The vacuum level during operation of the thruster is also important. In our case it is at most $5x10^{-5}$ mbar, which is often lower than the other experiments in literature, and may lead to the better performance.

Table 1 Performances of ECR plasma thruster operated with xenon

$\dot{m}_{Xe}$ [mg/s]	P [W]	I_i [mA]	E_i [eV]	T [mN]	I_{sp} [s]	I_{sp_ion} [s]	η_m	η_e	η_D	η_T
0.06	40	11.2	350	0.29	488	2298	26.2%	11%	79%	1.7%
0.1	33	26.5	215	0.45	454	1801	36.5%	17%	70%	3.0%
0.1	51	29.7	280	0.58	585	2055	40.9%	16%	70%	3.3%
0.2	34	49.0	110	0.59	298	1288	33.7%	16%	69%	2.5%
0.2	51	65.4	125	0.85	429	1373	45.1%	16%	70%	3.5%
0.3	51	80.3	90	0.86	289	1165	36.7%	14%	70%	2.4%

Table 2 Performances of ECR plasma thruster operated with argon

$\dot{m}_{Ar}$ [mg/s]	P [W]	I_i [mA]	E_i [eV]	T [mN]	I_{sp} [s]	I_{sp_ion} [s]	η_m	η_e	η_D	η_T
0.1	45	29.4	235	0.31	313	3420	12.2%	15%	75%	1.07%
0.2	47	66.7	125	0.5	252	2500	13.9%	18%	73%	1.33%

The specific impulse in Table 1 is calculated from the estimated thrust and the propellant gas mass flow, while I_{sp_ion} is the ideal specific impulse, *i.e.* the I_{sp} that would be achieved for an axial beam of ions with a mass utilization efficiency of 1. The best specific impulse (at 0.1 mg/s and 51 W) is close to 600 s, but higher I_{sp} (>2000 s) could theoretically be obtained by improving the mass utilization efficiency and the divergence factor. The ECR thruster efficiency remains quite low (less than 4%) in comparison with a Hall Effect Thruster or a Gridded Ion Engine. However, according to studies on xenon thrusters, the mass utilization efficiency can be increased by a factor of 2, and a significant improvement of the energy efficiency can be expected by optimizing the electric field amplitude in the microwave cavity (amplitude of the electric field) and the configuration of the magnetic field to reduce losses of ions on the walls.

VI. Conclusion

In this paper, we have described an electron cyclotron resonance (ECR) plasma thruster under development at ONERA, remarkable by the compact coaxial configuration of the ECR source and the purely divergent geometry of the applied magnetic field. The performances were evaluated in terms of ion current, ion energy and mass utilization efficiency using ion current density profiles and ion energy distributions measured with electrostatic probes. The ion current is seen to increase with microwave power, and mass utilization efficiencies as high as 45% have been achieved for a MW power of 51 W. The conversion of electron thermal energy into ion kinetic energy in the magnetic nozzle leads to the acceleration of Xe^+ ions up to several hundreds eV. It was found that the ion energy strongly decreases when the xenon mass flow rate is increased. The thrust was estimated at 0.85 mN with 0.2 mg/s of xenon. Better performances were obtained with xenon compared to argon, probably due to the lower ionization potential and larger ionization cross-section.

These promising results show the potential of the coaxial ECR thruster for spacecraft propulsion. Moreover, substantial improvements of the performances could be obtained by optimizing the thruster configuration. For instance, the mass utilization efficiency could be increased with a larger resonance region in the source. An optimization of the magnetic nozzle topology could also improve the ion acceleration.

Future works will include thrust measurements on ONERA microNewton thrust balance to verify electrostatic probes measurements. The measurement of the absolute ion velocity profile by laser induced fluorescence will provide crucial information for a better understanding of the ion acceleration mechanism.

Acknowledgments

This work was funded by Astrium and Thales Alenia Space France in the framework of the Next Generation Platform (NGP) project.

References

1 Charles, C., Boswell, R. W., and Lieberman, M. A., "Xenon ion beam characterization in a helicon double layer thruster", *Applied Physics Letter*, Vol. 89, No. 26, 2006.

2 Charles, C., "Plasmas for spacecraft propulsion", *Journal of Physics D: Applied Physics*, Vol. 42, No. 16, 2009.

3 Pavarin, D., et al., "Thruster Development Set-up for the Helicon Plasma Hydrazine Combined Micro Research Project (HPH.com)", *32nd International Electric Propulsion Conference*, Wiesbaden, Germany, 2011.

4 Wiebold, M., Sung, Y.-T., and Scharer, J.E., "Experimental observation of ion beams in the Madison Helicon eXperiment", *Physics of Plasmas*, Vol. 18, No. 6, 2011.

5 Batishchev, O., "Mini-Helicon Plasma Thruster Characterization", *AIAA 44th Joint Propulsion Conference*, Hartford, 2008.

6 Kammash, T., Tang, R., "Propulsive Capability of an Asymmetric GDM Propulsion System", *AIAA 42nd Joint Propulsion Conference*, Sacramento, 2006

7 Tang, R., Gallimore, A., and Kammash, T., "Design and Results of a Microwave-Driven Gasdynamic Mirror Experiment", *Journal of Propulsion and Power*, Vol. 29, No. 3, pp. 507-519, 2013.

8 Arefiev, A. V., and Breizman, B. N., "Ambipolar acceleration of ions in a magnetic nozzle", *Physics of Plasmas*, Vol. 15, No. 4, 2008.

9 Deline, C. A., Bengtson, R. D., Breizman, B. N., Tushentsov, M. R., Jones, J. E., Chavers, D. G., Dobson, C. C., and Schuettpelz, B. M., "Plume detachment from a magnetic nozzle", *Physics of Plasmas*, Vol. 16, No. 3, 2009.

10 Ahedo, E., and Merino, M., "On plasma detachment in propulsive magnetic nozzles", *Physics of Plasmas*, Vol. 18, No. 5, 2011.

11 Ahedo, E., and Merino, M., "Two-dimensional plasma expansion in a magnetic nozzle: Separation due to electron inertia", *Physics of plasmas*, Vol. 19, 2012.

12 Chang Diaz, F. R., "An Overview of the VASIMR Engine: High Power Space Propulsion with RF Plasma Generation and Heating", *Radio Frequency Power in Plasmas: 14th Topical Conference*, Oxnard, AIP Conference Proceedings 595, 2001.

13 Longmier, B. W., Cassady, L. D., Ballenger, M. G., Carter, M. D., Chang-Diaz, F. R., Glover, T. W., Ilin, A. V., McCaskill, G. E., Olsen, C. S., and Squire, J. P., "VX-200 Magnetoplasma Thruster Performance Results Exceeding Fifty-Percent Thruster Efficiency", *Journal of Propulsion and Power*, Vol. 27, No. 4, pp 915-920, 2011.

14 Miller, D. B., and Gibbons, E. F., "Experiments with an Electron Cyclotron Resonance Plasma Accelerator", *AIAA Journal*, Vol. 2, No. 1, pp. 35-41, 1964.

15 Miller, D.B., and Bethke, G. W., "Cyclotron Resonnace Thruster Design Techniques", *AIAA Journal*, Vol. 4, No. 5, pp. 835-840, 1966.

16 Kaufman, D.A., Goodwin, D.G., "Plume characteristics of an ECR plasma thruster", *27th International Electric Propulsion Conference*, Seattle, 1993.

17 Sercel, J. C., "Electron-Cyclotron-Resonance (ECR) Plasma Acceleration", *AIAA 19th Fluid Dynamics, Plasma Dynamics and Lasers Conference*, Hawaii, 1987.

18 Larigaldie, S., ONERA, France, French Patent for "Propulseur plasmique et procédé de génération d"une poussée propulsive plasmique", submitted 29 Dec. 2011.

19 Asmussen, J., Fritz, R., Mahoney, L., Fournier, G., and Demaggio, G., "ECR ion and free radical source for MBE applications", *Review of Scientific Instruments*, Vol. 61, No. 1, pp. 282-284, 1990.

20 Sitar, Z., Paisley, M. J., Smith, D. K., and Davis, R. F., "Design and performance of an electron resonance plasma source for standard molecular beam epitaxy equipment", *Review of Scientific Instruments*, Vol. 61, No. 9, pp. 2407-2411, 1990.

21 Baskaran, R., Jain, S. K., and Ramamurthy, S. S., "A compact coaxial electron cyclotron resonance plasma source", *Review of Scientific Instruments*, Vol. 67, No. 3, pp. 1243-1245, 1996.

22 Sortais, P., Lamy, T., Medard, J., Angot, J., and Latrasse, L., "Ultracompact/ultralow power electron cyclotron resonance ion source for multipurpose applications", *Review of Scientific Instruments*, Vol. 81, 2010.

23 Böhm, C., and Perrin, J., "Retarding-field analyzer for measurement of ion energy distributions and secondary electron emission coefficients in low-pressure radio frequency discharges", *Review of Scientific Instruments*, Vol. 64, No. 1, pp. 31-44, 1993.
24 Gueroult, R., Elias, P.-Q., Packan, D., and Rax, J.M., "A narrow-band, variable energy ion source derived from a wire plasma source", *Plasma Sources Science and Technology*, Vol. 20 , No. 4, 2011.
25 Goebel, D. M., and Katz, I., Fundamentals of Electric Propulsion: Ion and Hall Thrusters, JPL Space Science and Technologies Series, Wiley, 2008.
26 Takahashi, K., Lafleur, T., Charles, C., Alexander, P., Boswell, R. W., Perren, M., Laine, R., Pottinger, S., Lappas, V., Harle, T., and Lamprou, D., "Direct thrust measurement of a permanent magnet helicon double layer thrusters", *Applied Physics Letter*, Vol. 98, 2011.
27 Shabshelowitz, A., and Gallimore, A. D., "Performance and probe measurements of a radio-frequency plasma thruster", *Journal of Propulsion and Power*, Vol. 29, No. 4, pp. 919-929, 2013.